3. Strontium Isotope Stratigraphy of Cretaceous Sediments at Sites 1183 and 1186, Ontong Java Plateau[1]

Timothy J. Bralower,[2] Paul D. Fullagar,[3] Taylor A. McCay,[3] Kenneth G. MacLeod,[4] James Bergen,[5] and Eglée Zapata[6]

ABSTRACT

Strontium isotope stratigraphy of the Cretaceous sections recovered in Holes 1183A and 1186A generally matches trends expected from the seawater Sr isotope curve. Combined with biostratigraphic data, the $^{87}Sr/^{86}Sr$ measurements provide a good chronostratigraphic framework for these holes. In the mid-Cretaceous where the seawater Sr isotopic curve changes direction several times, biostratigraphy removes ambiguity in interpreting $^{87}Sr/^{86}Sr$ values. Furthermore, $^{87}Sr/^{86}Sr$ values refine the interpretation of several mid-Cretaceous unconformities suggested by nannofossil biostratigraphy. For the Campanian–Maastrichtian sediments in both holes, ages predicted from Sr isotope stratigraphy are as much as 2.5 m.y. younger than those from nannofossil stratigraphy. This offset likely results from differences in the way that ages are calibrated to nannofossil datums and the seawater Sr isotopic curve. Numerous Sr isotope values are high for their stratigraphic position, suggesting incorporation of excess ^{87}Sr presumably derived from terrigenous clays. Other Sr isotope values suggest minor errors in the estimated ages of nannofossil datums.

[2]Department of Geosciences, Pennsylvania State University, 503 Deike Building, University Park PA 16802, USA. **bralower@geosc.psu.edu**
[3]Department of Geological Sciences, University of North Carolina, Campus Box 3315, Mitchell Hall, Room 107, Chapel Hill NC 27599-3315, USA.
[4]Department of Geological Sciences, University of Missouri, 101 Geology Building, Columbia MO 65211-1380, USA.
[5]British Petroleum, 501 Westlake Park Boulevard, Houston TX 77079, USA.
[6]Department of Geology, Faculty of Engineering, Universidad Central de Venezuela, Caracas, Venezuela.

INTRODUCTION

A detailed understanding of the age and depositional history of the sediment column overlying basement is essential for achieving the principal objectives of Leg 192, which are understanding the eruptive history of the Ontong Java Plateau and its environmental consequences. The Maastrichtian to Aptian sections at Sites 1183 and 1186 were characterized by poor core recovery. In addition, difficulties in application of planktonic foraminiferal and nannofossil zonal markers, resulting from poor core recovery and fossil preservation, complicated correlation of the sections to other sequences from this interval, placement of stage boundaries, and estimates of absolute ages. Strontium isotope stratigraphy provides an independent source of age information that can help refine stratigraphic interpretations (e.g., Jenkyns et al., 1995; MacLeod et al., 2003).

The seawater Sr isotope curve ($^{87}Sr/^{86}Sr$ ratios) provides an independent chemostratigraphic means of correlation in marine sequences (e.g., McArthur et al., 2001). Marine carbonates, in particular, have been shown to faithfully record seawater Sr isotope ratios at deposition (Burke et al., 1982; DePaolo and Ingram, 1985). Moreover, because the ocean is well mixed with respect to Sr (the residence time of Sr in the ocean is on the order of 10^6 yr, whereas the mixing time is on the order of 10^3 yr), stratigraphic fluctuations in the Sr isotope composition of marine carbonate strata are globally synchronous (e.g., Veizer and Compston, 1974; Brass, 1976; Burke et al., 1982; Koepnick et al., 1985; Hess et al., 1986). For the parts of the timescale where the seawater Sr isotope curve is well established, Sr isotope stratigraphy can be used to provide age control in sediments that are difficult to date by other means, such as shallow-water carbonates (e.g., Ludwig et al., 1988; Jenkyns et al., 1995; Lehmann et al., 1999).

The seawater Sr isotope stratigraphy of the Cretaceous has been the subject of a number of detailed investigations. The similarity of stratigraphic changes recorded in different sections and on a variety of fossil groups and mineral types strongly suggests that the seawater Sr isotope curve for this period is robust and reproducible (e.g., McArthur et al., 1993, 1994, 2001; Jones et al., 1994; Huber et al., 1995; Sugarman et al., 1995; Bralower et al., 1997; Mearon et al., 2003). Much of the data collected has been integrated in the LOWESS curve, which provides a reference (McArthur et al., 2001) for estimating ages using Sr isotope measurements. In parts of the Cretaceous where seawater $^{87}Sr/^{86}Sr$ values changed rapidly, Sr isotopes can be used to provide important stratigraphic information in sections that are difficult to date because of poor core recovery and those that contain multiple unconformities.

Cretaceous sections recovered during Leg 192 present stratigraphic challenges that Sr isotope stratigraphy is well suited to address. The sections are composed of chalk and limestone containing microfossils that range from well to poorly preserved. In addition, recovery was low throughout most of the holes drilled. The combination of poor preservation in places and poor recovery made application of traditional microfossil biostratigraphies problematic, and these problems were compounded in the lower part of the Site 1183 section where nannofossil data suggest the presence of at least three unconformities (Sikora and Bergen, submitted [N1]).

METHODS

Because of the general lithified nature of the sediments, Sr isotope analyses were done on bulk material. All samples were powdered and dried. Approximately 5 mg of sample was dissolved in 500 µL of 1-M acetic acid and centrifuged. The supernatant was decanted and dried. The residue was then dissolved in 250 µL of 5-M HNO_3, loaded on a column containing 50 µL of Eichrom SrSpec resin, and washed with 600 µL of 5-M HNO_3. The Sr was eluted in 1 mL of H_2O. Total procedural blanks were ~200 pg Sr. Samples were loaded in $TaCl_5$ on single Re filaments and analyzed at the University of North Carolina at Chapel Hill on a Micromass Sector 54 thermal ionization mass spectrometer in dynamic mode. Fractionation was corrected using $^{86}Sr/^{88}Sr = 0.1194$.

During this study, $^{87}Sr/^{86}Sr$ analyses of 70 aliquots of Sr carbonate standard SRM 987 yielded an average value of 0.710263 ± 9 (2 standard deviations). Five to eight SRM987 aliquots were analyzed with each group of ~15 samples, and the average value for these replicates within each run was adjusted to 0.710250 to correct for possible instrument variation and to adjust results to those used to construct the seawater Sr curve (McArthur et al., 2001). For example, if the values for the standards analyzed with a group of samples averaged 0.710264, we subtracted 0.000014 from the $^{87}Sr/^{86}Sr$ ratio for each sample in that group. A total of 48 samples were analyzed, and 2 samples were analyzed in duplicate. Internal precision for Sr isotope analysis was typically 0.0006%–0.0009% standard error, based on 100 dynamic cycles of data collection.

Ages of samples are determined by plotting Sr isotope ratios on the correlative (determined using preliminary biostratigraphic data [Mahoney, Fitton, Wallace, et al., 2002]) portion of the LOWESS version 3 curve (McArthur et al., 2001). In the Santonian–Maastrichtian part of the section, Sr isotope values increase consistently with decreasing age and estimating ages from Sr measurements is straightforward. In the Aptian–Coniacian part of the section, however, where Sr isotope values both increase and decrease with age, application of biostratigraphy is often ambiguous and alternative age interpretations must be closely considered. For this interval, ages predicted by Sr isotope stratigraphy were compared in detail with those from nannofossil biostratigraphy. Selected datums that are well established and reliable are taken from Sikora and Bergen (submitted [N1]). Ages of these nannofossil datums were taken from Bralower, Premoli Silva, Malone, et al. (2002).

RESULTS

Strontium isotope ratios of bulk samples from Holes 1183A and 1186A (Table T1) are plotted vs. depth (Figs. F1, F2) and converted to ages by plotting Sr isotope values on the LOWESS curve (McArthur et al., 2001) (Fig. F3). Age-depth curves generated using these age estimates are compared with nannofossil biostratigraphic datums for Holes 1183A and 1186A in Figures F4 and F5, respectively.

Strontium isotope values in Hole 1183A separate into three distinct stratigraphic groupings (Table T1; Figs. F1, F4):
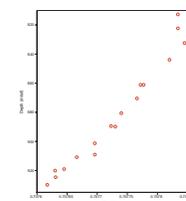
1. Between ~1130 and ~1112 meters below seafloor (mbsf), $^{87}Sr/^{86}Sr$ values suggest a late early Aptian (118.6 Ma) to early Albian
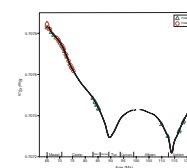
T1. Sr isotopic data, Holes 1183A and 1186A, p. 16.

F1. $^{87}Sr/^{86}Sr$ values vs. depth, Hole 1183A, p. 11.
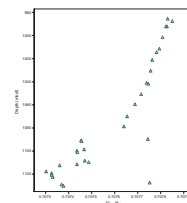
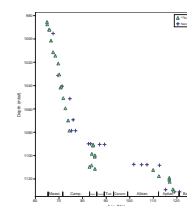**F2.** $^{87}Sr/^{86}Sr$ values vs. depth, Hole 1186A, p. 12.

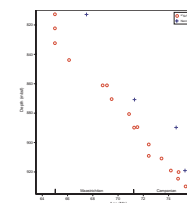**F3.** $^{87}Sr/^{86}Sr$ ages, Holes 1183A and 1186A, p. 13.

F4. $^{87}Sr/^{86}Sr$ ages, Hole 1183A, p. 14.

F5. $^{87}Sr/^{86}Sr$ ages, Hole 1186A, p. 15.

(109.9 Ma) age; from ~1130 to ~1118 mbsf values decrease from 0.707377 to 0.707302 and then increase to 0.707361 at 1112.36 mbsf;

2. Between 1111 mbsf and 1091 mbsf $^{87}Sr/^{86}Sr$ values lie between 0.707436 and 0.707454 and suggest an early (85.2 Ma) to late (84.5 Ma) Santonian age;

3. Between 1079 and 985 mbsf, values increase from 0.707640 to 0.707830, consistent with a late Campanian (74.4 Ma) to latest Maastrichtian (65.0 Ma) age.

Three anomalously high $^{87}Sr/^{86}Sr$ values were measured in Samples 192-1183A-50R-1, 133–136 cm ($^{87}Sr/^{86}Sr$ = 0.707744), 50R-2, 37–40 cm (0.707945), and 54R-1, 50–51 cm (0.707752) (Fig. F1; these values are not included in other figures).

Strontium isotope values in Hole 1186A correspond closely to the youngest stratigraphic group recognized in Hole 1183A. Values increase linearly from 0.707617 at 930 mbsf to 0.707845 at 832 mbsf, and, as in Hole 1183A, the highest sample(s) have slightly lower Sr isotope values than a subjacent sample (Table T1; Figs. F2, F5). In both cases the apparent latest Maastrichtian decrease is small and results from higher values in only one or two samples; however, latest Maastrichtian decreases have also been reported in Nelson et al. (1991), Martin and Macdougall (1991), Vonhof and Smit (1997), McArthur et al. (1998), and MacLeod et al. (2003).   Predicted ages from $^{87}Sr/^{86}Sr$ for the studied section in Hole 1186A range from late Campanian (75.4 Ma) to latest Maastrichtian (65.0 Ma).

DISCUSSION

Strontium isotope stratigraphy has the potential to provide important age information, especially in sections where deep burial, poor core recovery, and/or lack of age-diagnostic microfossils have confounded stratigraphic interpretation. However, before Sr isotope stratigraphy and the ages predicted from it can be accepted, the extent of diagenetic alteration must be assessed.

Diagenetic alteration is known to affect original Sr isotope values of carbonates as a result of exchange with pore fluids during recrystallization. Minor alteration in sediments with a significant clay component that often possess a highly radiogenic Sr isotope signature can have a relatively large effect on the final $^{87}Sr/^{86}Sr$ ratio (e.g., Bralower et al., 1997; Mearon et al., 2003). For chalks and limestones that are nearly pure biogenic carbonate, major recrystallization usually has a relatively small effect on Sr isotope ratios, as the system is well buffered to contemporary seawater values. However, these small effects can translate into significant age errors (i.e., 1–2 m.y.) in parts of the section such as the Campanian where $^{87}Sr/^{86}Sr$ values change slowly through time. Moreover, even minor amounts of clay can impart a radiogenic signature during recrystallization. When analyses of these sediments are made on components such as foraminifers, the effect of recrystallization can be gauged by scanning electron microscopy (Bralower et al., 1997); with bulk carbonate analyses such discrimination is impossible, and diagenetic concerns can only be addressed indirectly.

One indicator of potential diagenetic alteration of Sr isotope ratios is the occurrence of visible residue, often composed of clay, after carbonate samples are dissolved. An alternate method of gauging the effect of

T.J. Bralower, et al.
Strontium Isotope Stratigraphy

5

diagenesis on Sr isotopic values is by comparison of predicted ages with those obtained from biostratigraphy. Consistent offsets between biostratigraphy and Sr isotope stratigraphy can arise from differences in the way absolute ages are assigned to biostratigraphic datums and the seawater Sr isotopic curve; alternatively, such offsets may be an indication of diagenetic alteration. Because more indurated samples are more likely to have experienced minor alteration of Sr ratios during recrystallization, analysis of lithology can explain deviation of results from those expected from stratigraphy. In Hole 1183A, where samples span a considerable depth range (Table T1) and lithology gradually changes downward from chalk to limestone over the course of this interval, the scatter increases downsection as does the deviation from Sr isotope values expected from biostratigraphy (Figs. F1, F3).

Ages of nannofossil datums used here were calculated using the Gradstein et al. (1994) timescale, assuming constant sedimentation rates in key sections in the pre-Campanian and combining this assumption with ages of magnetic chrons in the Campanian and Maastrichtian (e.g., Bralower, Premoli Silva, Malone, et al., 2002). Ages of Sr isotope values used to derive the LOWESS curve (McArthur et al., 2001) are taken directly from publications and calibrated to the Gradstein et al. (1994) timescale. The biostratigraphy on which the Cretaceous part of the LOWESS curve is based includes nannofossils (Bralower et al., 1997; McArthur et al., 1993) and a range of macrofossils (ammonites, belemnites, and bivalves [e.g., McArthur et al., 1993, 1994; Jones et al., 1994]). Part of the LOWESS curve is directly calibrated with bentonite radiometric ages (e.g., McArthur et al., 1994), but in other cases ages are derived from stage boundary identifications in the sections studied (McArthur et al., 1993) and from zonal boundary ages determined assuming constant sedimentation rates (e.g., Bralower et al., 1997) and constant ammonite zonal durations (e.g., Jones et al., 1994).

Finally, a limitation exists in the mid-Cretaceous where an Sr isotope value on its own might indicate two or three different ages. This uncertainty exists because the seawater Sr isotopic curve changes direction several times (Fig. F3). In this interval, paleontological or other stratigraphic data are necessary to constrain the possible ages to a small portion of the seawater curve and allow a unique age to be predicted from Sr isotope stratigraphy. In this case, Sr isotope data can then be used to provide a more precise age estimate and test for minor errors in biostratigraphic ages, but circularity becomes a problem in addressing stage-level questions.

In Hole 1183A, predicted ages from Sr isotope values agree moderately well with ages from nannofossil biostratigraphy (Fig. F4). In the Campanian–Maastrichtian section, predicted ages are similar to or slightly (~2 m.y.) younger than biostratigraphic ages. Part of the offset could result from minor variations in $^{87}Sr/^{86}Sr$ that are a result of recrystallization. These minor offsets are also possibly a result of uncertainty in age estimates derived from nannofossil biostratigraphy, combined with differences in the way absolute ages are calculated from nannofossil biostratigraphy and Sr isotope stratigraphy. Similar offsets between predicted and biostratigraphic ages also occur at Ocean Drilling Program Sites 738, 1049, 1050, and 1052, suggesting that the ages of datums used to calibrate LOWESS are too low or those estimated for the nannofossil datums are too high. A possible explanation for this is that the LOWESS curve in this interval is hinged on boreal and western interior macrofossil (e.g., McArthur et al., 1993, 1994) and microfossil (e.g., Burnett [1990], used in McArthur et al. [1993]) zones, which may be

systematically offset from stage boundary definitions in the deep-sea sites based on microfossil zones. For example, the one common nannofossil datum used by Burnett (1990) that is found routinely in the deep-sea sites, the first occurrence (FO) of *Aspidolithus parcus*, lies in the middle lower Campanian in the former study but close to the Santonian/Campanian boundary in Bralower, Premoli Silva, Malone, et al. (2002) and other publications. This difference would lead to the observed offset whereby predicted ages from LOWESS are younger than those from nannofossil biostratigraphy.

More significant disparities exist in the section between 1090 and 1130 mbsf, where nannofossil biostratigraphy suggests at least three unconformities (Sikora and Bergen, submitted [N1]). The first occurs at ~1090 mbsf and spans ~7 m.y. from the early Campanian (82.5 Ma) to the latest Turonian (89.3 Ma); the second, at ~1108 mbsf, spans ~11 m.y. from the late Albian to the latest Aptian (101.7–112.6 Ma); and the third, near the sediment/basement contact at ~1130.37 mbsf, spans ~2 m.y. from the early Aptian (119.0 Ma) to the latest Barremian (121.1 Ma). Sr isotope values suggest breaks in sedimentation at two of these levels (likely hiatuses of ~10 m.y. between ~1079 [74.38 Ma] and 1090 mbsf [84.49 Ma] and ~25 m.y. at ~1112 mbsf [85.2–109.9 Ma]). On the other hand, Sr isotope data suggest a relatively thick Santonian section at 1091–1111 mbsf and an apparently continuous lower Albian to upper lower Aptian section at 1112–1130 mbsf and do not confirm the lowest of the three proposed hiatuses.

The lowermost hiatus indicated by nannofossil biostratigraphy in Hole 1183A may be an artifact of the truncation of ranges near the sediment/basement contact. The FOs of *Hayesites irregularis* and *Eprolithus floralis* lie immediately above basement and may not reflect true datum levels. The FO of *Rhagodiscus achlyostaurion*, just over 1 m above basement, may also be unreliable because of disparities between the taxonomies of different workers who have applied this datum (e.g., Erba, 1991; Bralower et al., 1993; Bergen, 1994; Tremolada, 2002). Thus, Sr isotope stratigraphy may provide a more precise age interpretation of the lowermost 18 m of section in Hole 1183A.

The hiatus at ~1108 mbsf indicated by nannofossil biostratigraphy is based on several well-established and reliable datums including the FOs of *Prediscosphaera columnata* and *Eiffellithus turriseiffelii*. These datums are inconsistent with Sr isotope values of three samples between 1108 and 1111 mbsf (Fig. F4). Two of these samples contained dark residues after dissolution, possibly reflecting a contribution of radiogenic Sr from clays that increased their Sr isotope values above original seawater levels. The 1090-mbsf unconformity corresponds to the FOs of *Marthasterites furcatus, Micula staurophora, Aspidolithus parcus parcus,* and *Aspidolithus parcus constrictus*. The FOs of the latter two datums fit well with Sr isotope stratigraphy, but the FOs of *M. furcatus* and *M. staurophora* are inconsistent with Sr isotope values of the three samples between 1098 and 1101 mbsf. These samples contain higher Sr isotope values than predicted by nannofossil biostratigraphy, and two of them had a dark residue after dissolution. One, however, did not, and the other sample with similar residues matches expected values; thus, it is difficult to dismiss these values as diagenetic artifacts. An alternative explanation is that the disparity arises from differences in the stratigraphic position of *M. staurophora* in different timescales and the paucity of specimens of *M. furcatus* toward the base of its range in Hole 1183A.

In the Campanian–Maastrichtian interval of Hole 1186A, predicted ages from Sr isotope values are as much as ~2.5 m.y. younger than ages

from nannofossil biostratigraphy, about the same magnitude as disparities in this part of the section in Hole 1183A (Figs. F4, F5). These disparities are likely a result of minor recrystallization combined with differences in the way that absolute ages are calibrated to nannofossil datums and the LOWESS curve. The disparity between ages predicted by Sr isotope stratigraphy and biostratigraphy at ~813 mbsf likely results from the truncation of the range of *Lithraphidites quadratus* at the Cretaceous/Paleocene unconformity (Mahoney, Fitton, Wallace, et al., 2001).

CONCLUSIONS

Strontium isotope stratigraphy of samples from Holes 1183A and 1186A combined with biostratigraphic data provide a good stratigraphic framework for the mid- to Late Cretaceous sections recovered during Leg 192. Sr isotope stratigraphy suggests that the section recovered in Hole 1183A consists of an upper lower Aptian to lower Albian interval separated by an unconformity from a Santonian interval that unconformably underlies a thick upper Campanian to upper Maastrichtian interval. The section recovered at the top of Hole 1186A also consists of a relatively expanded upper Campanian to upper Maastrichtian interval.

ACKNOWLEDGMENTS

REFERENCES

Bergen, J.A., 1994. Berriasian to early Aptian calcareous nannofossils from the Vocontian Trough (SE France) and Deep Sea Drilling Site 534: new nannofossil taxa and a summary of low-latitude biostratigraphic events. *J. Nannoplankton Res.,* 16:59–69.

Bralower, T.J., Fullagar, P.D., Paull, C.K., Dwyer, G.S., and Leckie, R.M., 1997. Mid-Cretaceous strontium-isotope stratigraphy of deep-sea sections. *Geol. Soc. Am. Bull.,* 109:1421–1442.

Bralower, T.J., Premoli Silva, I., Malone, M.J., et al., 2002. *Proc. ODP, Init. Repts.,* 198 [Online]. Available from World Wide Web: <http://www-odp.tamu.edu/publications/198_IR/198ir.htm>. [Cited 2003-09-26].

Bralower, T.J., Sliter, W.V., Arthur, M.A., Leckie, R.M., Allard, D.J., and Schlanger, S.O., 1993. Dysoxic/anoxic episodes in the Aptian-Albian (Early Cretaceous). *In* Pringle, M.S., Sager, W.W., Sliter, W.V., and Stein, S. (Eds.), *The Mesozoic Pacific: Geology, Tectonics, and Volcanism.* Geophys. Monogr., Am. Geophys. Union, 77:5–37.

Brass, G.W., 1976. The variation of the marine $^{87}Sr/^{86}Sr$ ratio during Phanerozoic time: interpretations using a flux model. *Geochem. Cosmochim. Acta,* 40:721–730.

Burke, W.H., Denison, R.E., Hetherington, E.A., Koepnick, R.B., Nelson, H.F., and Otto, J.B., 1982. Variation of seawater $^{87}Sr/^{86}Sr$ throughout Phanerozoic time. *Geology,* 10:516–519.

Burnett, J.A., 1990. A new nannofossil zonation scheme for the Boreal Campanian. *INA Newsl.,* 12:67–70.

DePaolo, D.J., and Ingram, B.L., 1985. High-resolution stratigraphy with strontium isotopes. *Science,* 227:938–941.

Erba, E., 1991. Calcareous nannofossil distribution in pelagic rhythmic sediments (Aptian-Albian Piobbico core, Central Italy). *Riv. Ital. Paleontol. Stratigr.,* 97:455–484.

Gradstein, F.M., Agterberg, F.P., Ogg, J.G., Hardenbol, J., van Veen, P., Thierry, J., and Huang, Z., 1994. A Mesozoic time scale. *J. Geophys. Res.,* 99:24051–24074.

Hess, J., Bender, M.L., and Schilling, J.G., 1986. Evolution of the ratio of strontium-87 to strontium-86 in seawater from Cretaceous to present. *Science,* 231:979–984.

Huber, B.T., Hodell, D.A., and Hamilton, C.P., 1995. Mid- to Late Cretaceous climate of the southern high latitudes: stable isotopic evidence for minimal equator-to-pole thermal gradients. *Geol. Soc. Am. Bull.,* 107:1164–1191.

Jenkyns, H.C., Paull, C.K., Cummins, D.I., and Fullagar, P.D., 1995. Strontium-isotope stratigraphy of Lower Cretaceous atoll carbonates in the Mid-Pacific Mountains. *In* Winterer, E.L., Sager, W.W., Firth, J.V., and Sinton, J.M. (Eds.), *Proc. ODP, Sci. Results,* 143: College Station, TX (Ocean Drilling Program), 89–97.

Jones, C.E., Jenkyns, H.C., Coe, A.L., and Hesselbo, S.P., 1994. Strontium isotopic variations in Jurassic and Cretaceous seawater. *Geochim. Cosmochim. Acta,* 58:3061–3074.

Koepnick, R.B., Burke, W.H., Denison, R.E., Hetherington, E.A., Nelson, H.F., Otto, J.B., and Waite, L.E., 1985. Construction of the seawater $^{87}Sr/^{86}Sr$ curve for the Cenozoic and Cretaceous: supporting data. *Chem. Geol. (Isotope Geosci. Sect.),* 58:55–81.

Lehmann, C., Osleger, D.A., Montañez, I.P., Sliter, W.V., Arnaud-Vanneau, A., and Banner, J.L., 1999. Evolution of Cupido and Coahuila carbonate platforms, Early Cretaceous, northeastern Mexico. *Geol. Soc. Am. Bull.,* 111:1010–1029.

Ludwig, K.R., Halley, R.B., Simmons, K.R., and Peterman, Z.E., 1988. Strontium-isotope stratigraphy of Enewetak atoll. *Geology,* 16:173–177.

MacLeod, K.G., Fullagar, P.D., and Huber, B.T., 2003. $^{87}Sr/^{86}Sr$ test of the degree of impact-induced slope failure in the Maastrichtian of the western North Atlantic. *Geology,* 31:311–314.

Mahoney, J.J., Fitton, J.G., Wallace, P.J., et al., 2001. *Proc. ODP, Init. Repts.,* 192 [Online]. Available from World Wide Web: <http://www-odp.tamu.edu/publications/192_IR/192ir.htm>. [Cited 2003-09-26].

Martin, E.E., and Macdougall, J.D., 1991. Seawater Sr isotopes at the Cretaceous/Tertiary boundary. *Earth Planet. Sci. Lett.,* 104:166–180.

McArthur, J.M., Howarth, R.J., and Bailey, T.R., 2001. Strontium isotope stratigraphy: LOWESS version 3: best fit to the marine Sr-isotope curve for 0–509 Ma and accompanying look-up table for deriving numerical age. *J. Geol.,* 109:155–170.

McArthur, J.M., Kennedy, W.J., Chen, M., Thirlwall, M.F., and Gale, A.S., 1994. Strontium isotope stratigraphy for Late Cretaceous time: direct numerical calibration of the Sr isotope curve based on the US Western Interior. *Palaeogeogr., Palaeoclimatol., Palaeoecol.,* 108:95–119.

McArthur, J.M., Thirlwall, M.F., Engkilde, M., Zinsmeister, W.J., and Howarth, R.J., 1998. Strontium isotope profiles across the K/T boundary in Denmark and Antarctica. *Earth Planet. Sci. Lett.,* 160:179–192.

McArthur, J.M., Thirlwall, M.F., Gale, A.S., Kennedy, W.J., Burnett, J.A., Mattey, D., and Lord, A.R., 1993. Strontium isotope stratigraphy for the Late Cretaceous: a new curve, based on the English Chalk. *In* Hailwood, E., and Kidd, R. (Eds.), *High Resolution Stratigraphy.* Geol. Soc. Spec. Publ., 70:195–209.

Mearon, S., Paytan, A., and Bralower, T.J., 2003. Cretaceous strontium isotope stratigraphy using marine barite. *Geology,* 31:15–18.

Nelson, B.K., MacLeod, G.K., and Ward, P.D., 1991. Rapid change in strontium isotopic composition of sea water before the Cretaceous/Tertiary boundary. *Nature,* 351:644–647.

Sugarman, P.J., Miller, K.G., Bukry, D., and Feigenson, M.D., 1995. Uppermost Campanian-Maestrichtian strontium isotopic, biostratigraphic, and sequence stratigraphic framework of the New Jersey Coastal Plain. *Geol. Soc. Am. Bull.,* 107:19–37.

Tremolada, F., 2002. Aptian to Campanian calcareous nannofossil biostratigraphy from the Bottaccione section, Gubbio, Central Italy. *Riv. Ital. Paleontol. Stratigr.,* 108:441–456.

Veizer, J., and Compston, W., 1974. $^{87}Sr/^{86}Sr$ composition of seawater during the Phanerozoic. *Geochim. Cosmochim. Acta,* 38:1461–1484.

Vonhof, H.B., and Smit, J., 1997. High-resolution late Maastrichtian–early Danian oceanic $^{87}Sr/^{86}Sr$ record: implications for Cretaceous/Tertiary boundary events. *Geology,* 25:347–350.

Zapata, E., Padron, V., Madrid, I., Kertznus, V., Truskowski, I., and Lorente, M.A., in press. Biostratigraphic, sedimentologic and chemostratigraphic study of the La Luna formation (late Turonian–Campanian) in the San Miguel and Las Hernández Sections, Western Venezuela. *Palaios.*

APPENDIX

Strontium Isotope Stratigraphy of the La Luna Formation, Western Venezuela

This paper illustrates an example of the application of Sr isotope stratigraphy in refining interpretation of sections with equivocal stratigraphy derived from other techniques. Here we illustrate an example of Sr isotope stratigraphy that has clearly provided incorrect age information. We analyzed 61 samples from the La Luna Formation from the Las Hernández and San Pedro del Rio sections in the Venezuelan Andes. Biostratigraphy indicates that the section ranges from early Coniacian to early Campanian (Zapata et al., in press). Sr isotope ratios of the samples vary from 0.707507 to 0.708483, considerably higher than those for the age of the section determined by biostratigraphy (Table AT1; Fig. AF1). The range of Sr isotope values corresponds to the early Campanian–Miocene part of the seawater Sr isotope curve (McArthur et al., 2001). This range excludes all but the youngest interval predicted by biostratigraphy, indicating that the Sr isotope values are not those of original seawater. The samples are clay-rich and enriched in organic carbon (Table AT1). Residues after dissolution were dark colored, and it is likely that Sr isotope values were increased by inheritance of radiogenic Sr from noncarbonate components during recrystallization.

AT1. Sr isotope data, La Luna Formation, p. 18.

AF1. ^{87}Sr/^{86}Sr values, La Luna Formation, p. 17.
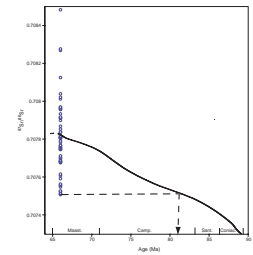
Figure F1. ^{87}Sr/^{86}Sr values vs. depth in Hole 1183A. Three anomalous data points are excluded from further consideration.
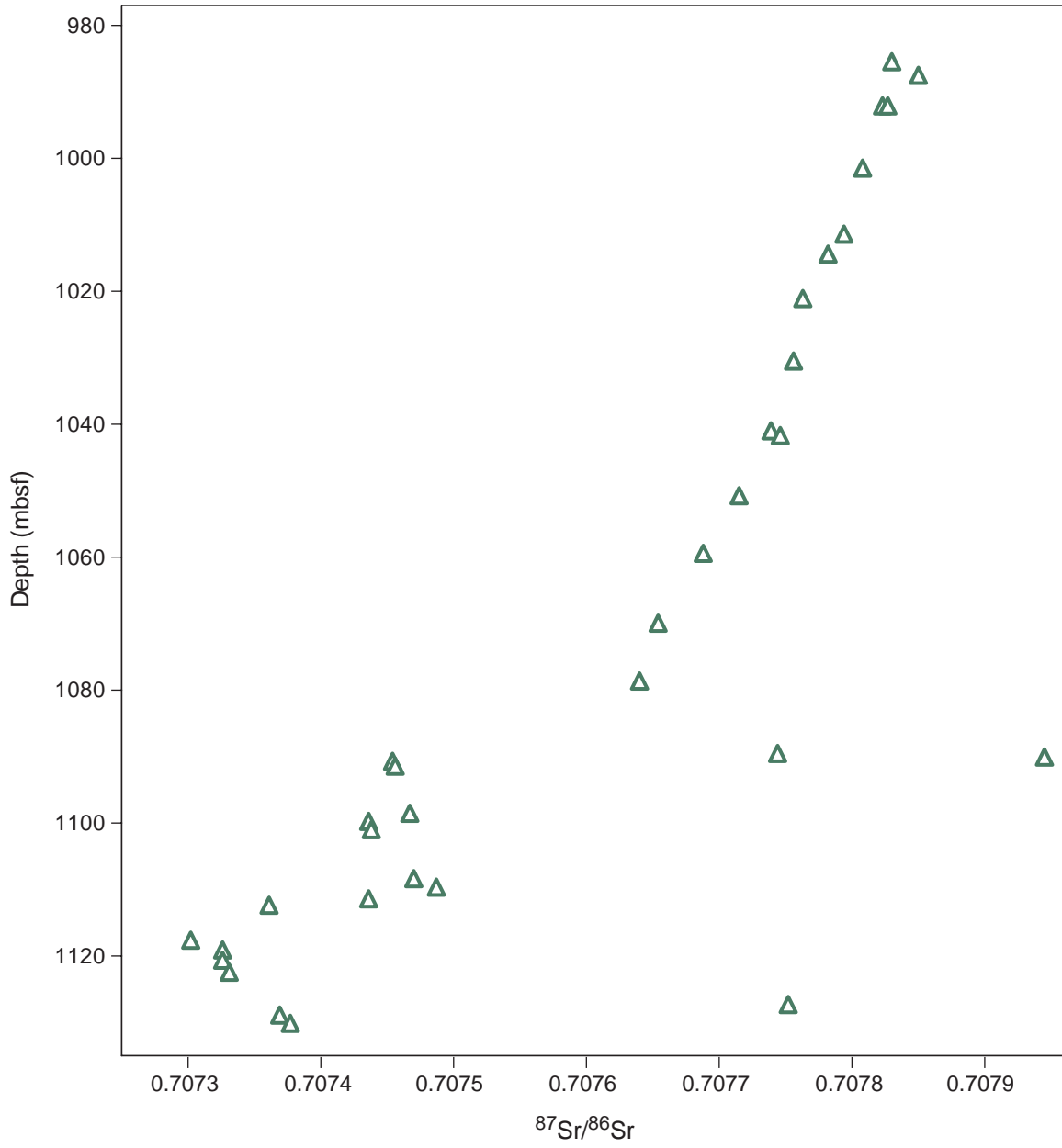
Figure F2. $^{87}Sr/^{86}Sr$ values vs. depth in Hole 1186A.
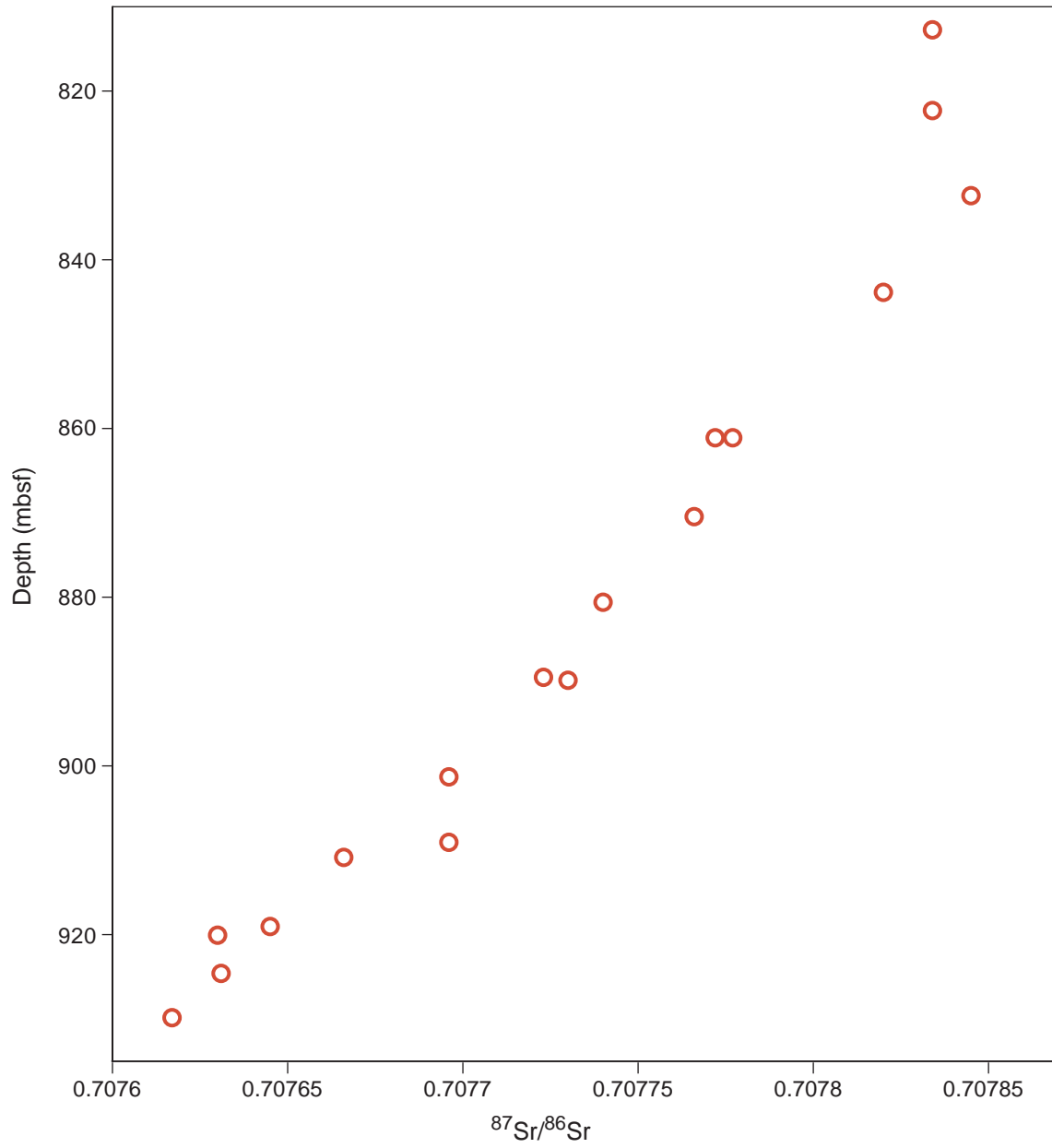
Figure F3. Age of samples from Holes 1183A and 1186A predicted from $^{87}Sr/^{86}Sr$ values and the LOWESS curve of McArthur et al. (2001). See text for full explanation.

Figure F4. Age of samples from Hole 1183A predicted from $^{87}Sr/^{86}Sr$ values and the LOWESS curve of McArthur et al. (2001) plotted vs. depth. See text for full explanation.

Figure F5. Age of samples from Hole 1186A predicted from $^{87}Sr/^{86}Sr$ values and the LOWESS curve of McArthur et al. (2001) plotted vs. depth. See text for full explanation.

Table T1. Sr isotopic data of samples, Holes 1183A and 1186A.

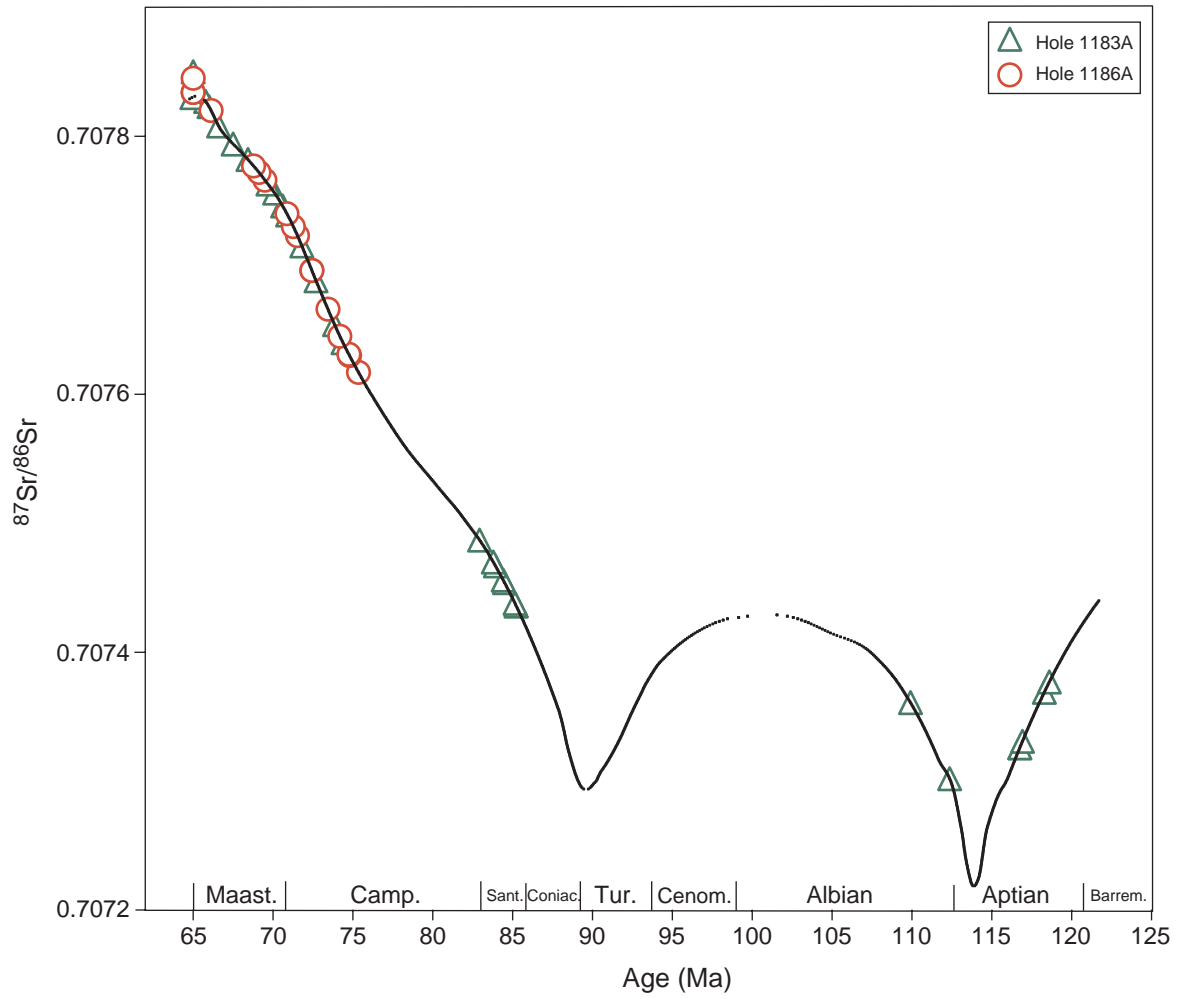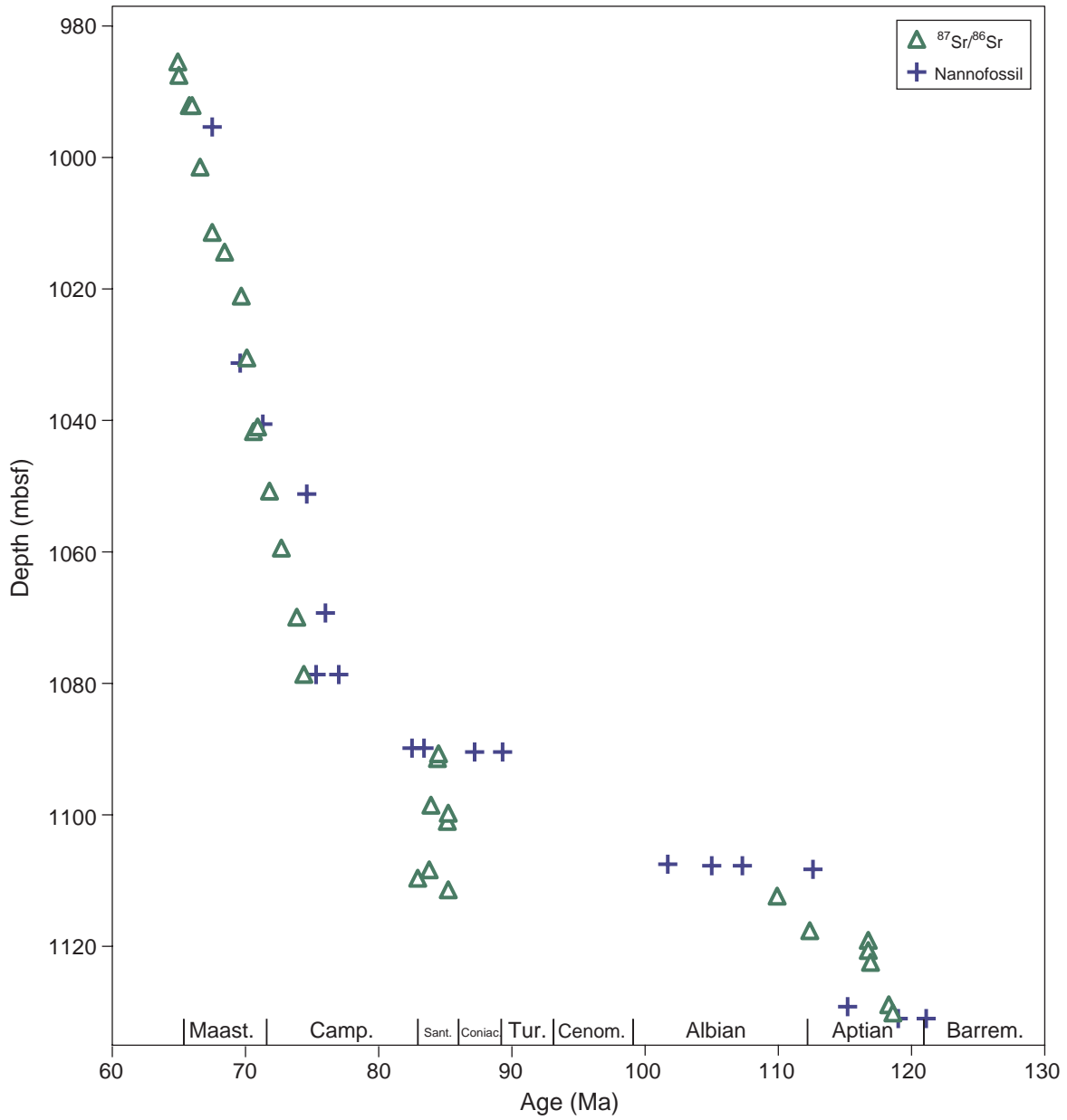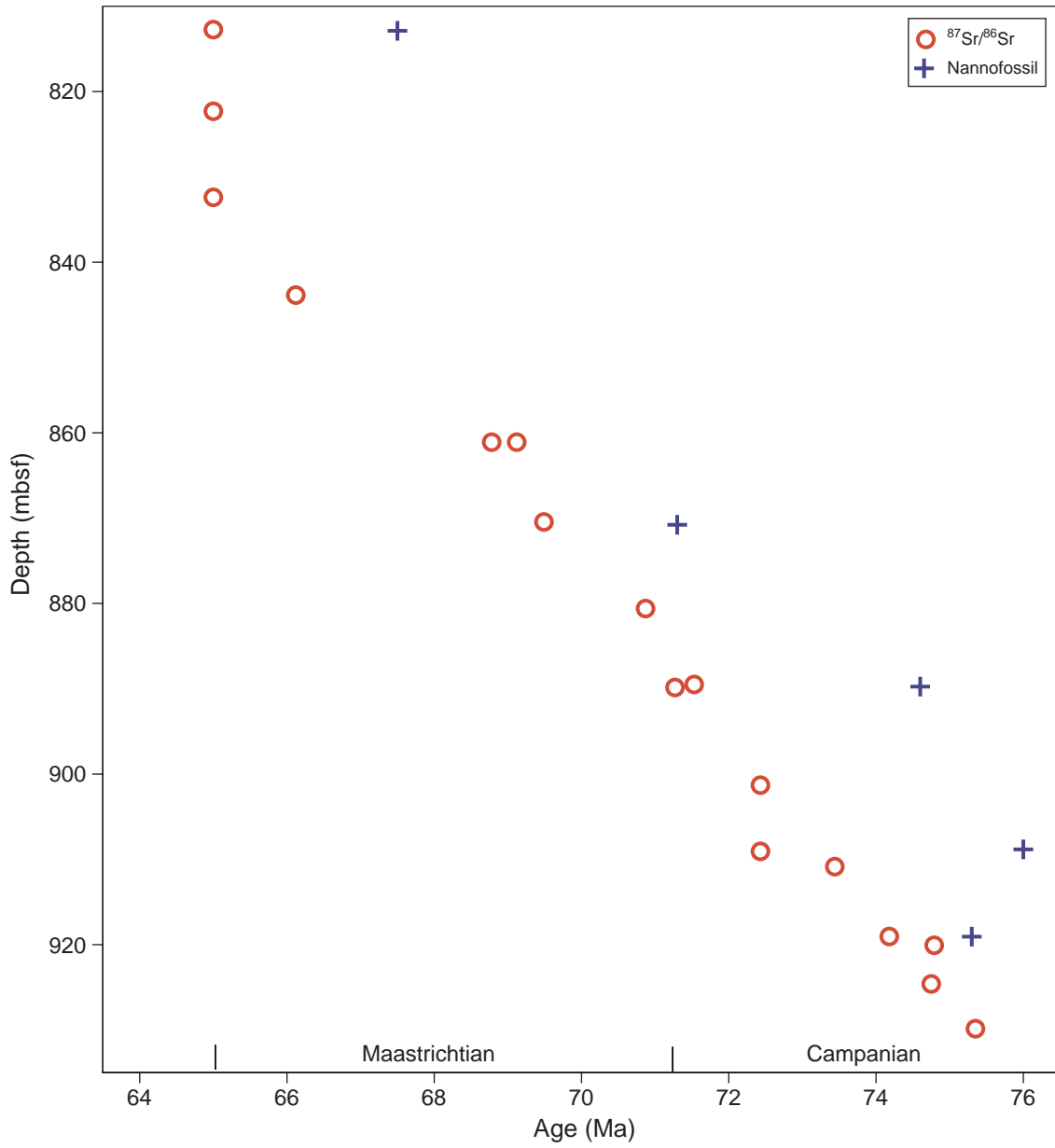| Core, section, interval (cm)	Depth (mbsf)	$^{87}Sr/^{86}Sr$	Standard error (±%)	Predicted age (Ma)	Comments
192-1183A-					
39R-3, 46–47	985.46	0.707830	0.0008	64.92	
39R-5, 0–1	987.51	0.707850	0.0006	65.00	
40R-1, 40–41	992.10	0.707827	0.0007	65.78	
40R-1, 40–41	992.10	0.707823	0.0009	65.99	Replicate
41R-1, 7–8	1001.47	0.707808	0.0008	66.59	
42R-1, 30–31	1011.40	0.707794	0.0008	67.50	
42R-3, 30–31	1014.40	0.707782	0.0007	68.43	
43R-1, 29–30	1021.09	0.707763	0.0008	69.68	
44R-1, 9–10	1030.49	0.707756	0.0007	70.10	
45R-1, 99–100	1040.99	0.707739	0.0008	70.91	
45R-2, 20–21	1041.70	0.707746	0.0008	70.60	
46R-1, 115–116	1050.75	0.707715	0.0006	71.80	
47R-1, 22–23	1059.42	0.707688	0.0007	72.69	
48R-1, 113–114	1069.93	0.707654	0.0006	73.85	
49R-CC, 13–14	1078.63	0.707640	0.0008	74.38	
50R-1, 133–136	1089.53	0.707744	0.0008	NA	
50R-2, 37–40	1090.07	0.707945	0.0007	NA	
50R-2, 101–104	1090.71	0.707454	0.0007	84.49	Dark residue
50R-3, 24–26	1091.44	0.707456	0.0008	84.41	
51R-1, 63–66	1098.53	0.707467	0.0006	83.92	
51R-2, 32–35	1099.75	0.707436	0.0008	85.22	Dark residue
51R-3, 10–12	1101.00	0.707438	0.0007	85.15	Dark residue
52R-1, 86–88	1108.36	0.707470	0.0008	83.79	Dark residue
52R-2, 64–66	1109.64	0.707487	0.0007	82.93	
52R-3, 90–93	1111.40	0.707436	0.0008	85.22	Dark residue
52R-4, 36–38	1112.36	0.707361	0.0007	109.91	Light brown residue
53R-1, 42–44	1117.62	0.707302	0.0009	112.36	
53R-2, 42–45	1119.09	0.707326	0.0006	116.75	
53R-3, 46–49	1120.63	0.707326	0.0005	116.75	Dark residue
53R-4, 100–102	1122.44	0.707331	0.0008	116.92	
54R-1, 50–51	1127.30	0.707752	0.0007	NA	
54R-2, 59–61	1128.89	0.707369	0.0007	118.29	
54R-3, 96–99	1130.13	0.707377	0.0007	118.60	Brown residue
192-1186A-					
14R-CC, 4–6	812.74	0.707834	0.0008	65.00	
15R-CC, 1–2	822.31	0.707834	0.0007	65.00	
16R-1, 40–42	832.40	0.707845	0.0007	65.00	
17R-2, 66–69	843.86	0.707820	0.0006	66.12	
19R-1, 50–51	861.10	0.707772	0.0008	69.12	
19R-1, 50–51	861.10	0.707777	0.0009	68.78	Replicate
20R-1, 25–26	870.45	0.707766	0.0007	69.49	
21R-1, 70–72	880.60	0.707740	0.0007	70.87	
21R-CC	889.50	0.707723	0.0007	71.53	
22R-1, 35–37	889.85	0.707730	0.0006	71.27	
23R-2, 70–72	901.30	0.707696	0.0005	72.43	
24R-1, 36–38	909.06	0.707696	0.0006	72.43	
24R-2, 65	910.85	0.707666	0.0007	73.44	
25R-1, 74–76	919.04	0.707645	0.0006	74.18	
25R-2, 27–29	920.07	0.707630	0.0007	74.79	
25R-5, 30–32	924.60	0.707631	0.0007	74.75	
26R-2, 35–36	929.85	0.707617	0.0008	75.35	

Note: NA = not available.

Figure AF1. ^{87}Sr/^{86}Sr values of samples from the La Luna Formation in the Las Henández Section, Venezuela (large circles) plotted against the Turonian–Maastrichtian part of the LOWESS curve of McArthur et al. (2001). See the "Appendix," p. 10, for discussion and Zapata et al. (in press) for details of stratigraphy. Dashed line refers to the oldest age indicated by Sr isotope values.
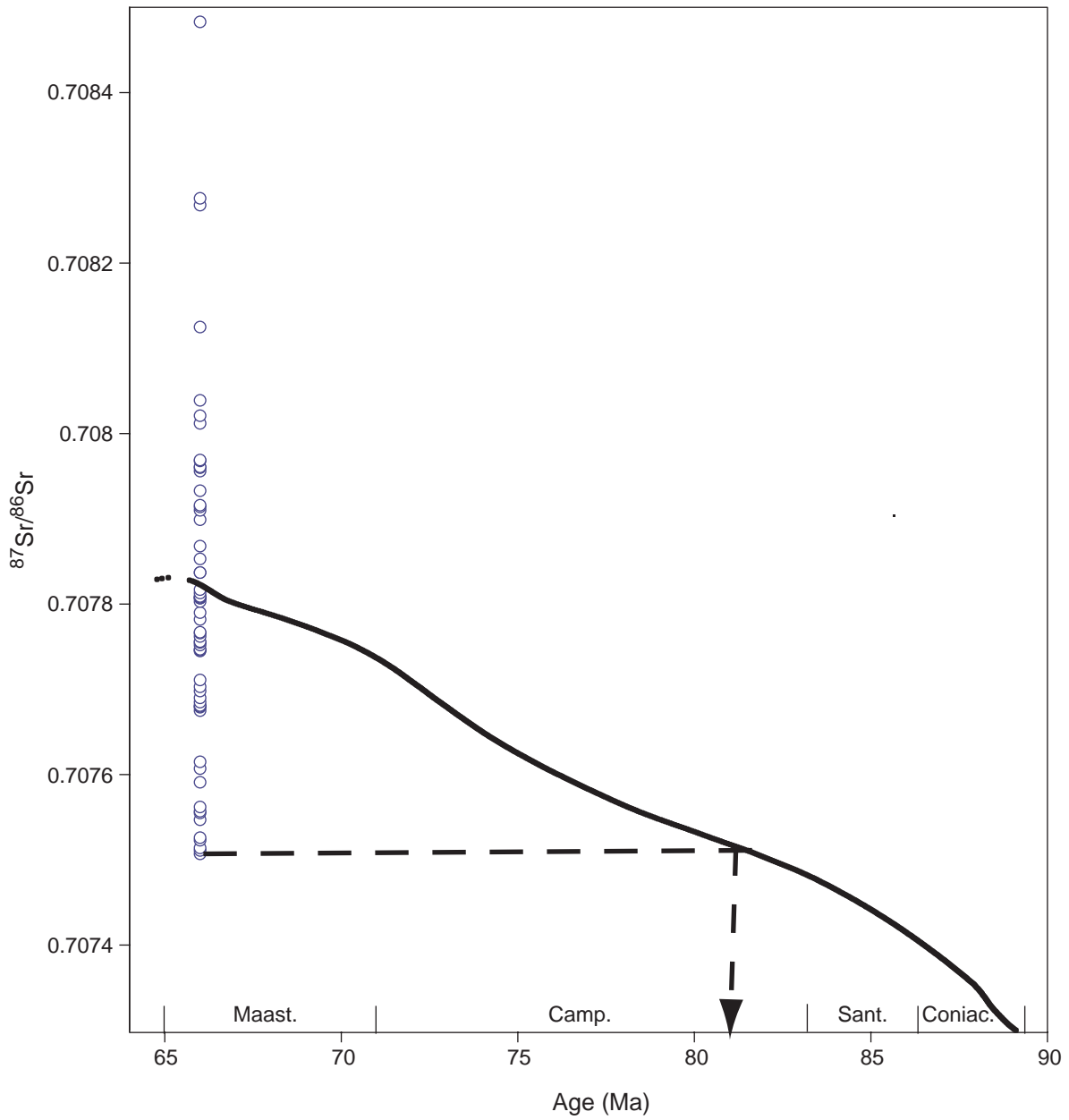
Table AT1. Sr isotope data, La Luna Formation, Venezuela.

Sample	$^{87}Sr/^{86}Sr$ (corrected)	Standard error (±%)	Carbon (wt%)	TOC (wt%)	Average of standards
Las Hernandez					
MLA 75(0.5)	0.707756	0.0008	95.27	1.28	0.710253
MLA 75(0.5)	0.707755	0.0007	95.27	1.28	0.710264
MLA 75(1.0)	0.707745	0.0008	95.27	1.28	0.710253
MLA 75(2.0)	0.707767	0.0015	95.27	1.28	0.710253
MLA 75(4.0)	0.707807	0.0018	95.27	1.28	0.710253
MLA 75(6.0)	0.707817	0.0014	95.27	1.28	0.710253
MLA 80(0.5)	0.707703	0.0006	97.49	0.66	0.710264
MLA 80(1.0)	0.707685	0.0007	97.49	0.66	0.710264
MLA 80(2.0)	0.707675	0.0008	97.49	0.66	0.710264
MLA 80(4.0)	0.707680	0.0010	97.49	0.66	0.710264
MLA 80(6.0)	0.707679	0.0010	97.49	0.66	0.710264
MLA 84(0.5)	0.707547	0.0007	95.51	4.11	0.710264
MLA 84(0.5)	0.707511	0.0009			0.710260
MLA 84(1.0)	0.707557	0.0008			0.710260
MLA 84(2.0)	0.707507	0.0008	95.51	4.11	0.710264
MLA 84(4.0)	0.707514	0.0008	95.51	4.11	0.710264
MLA 84(6.0)	0.707523	0.0156	95.51	4.11	0.710264
MLA 87	0.707615	0.0007	69.67	6.73	0.710252
MLA 92	0.707591	0.0007	83.34	1.16	0.710260
MLA 96	0.707607	0.0010	82.52	1.54	0.710260
MLA 101	0.707526	0.0008	96.46	2.48	0.710264
MLA 105	0.707690	0.0006	26.09	5.13	0.710260
MLA 108	0.707555	0.0007	98.40	2.56	0.710260
MLA 108	0.707562	0.0007			0.710260
MLA 112	0.707698	0.0010	45.25	2.72	0.710260
MLA 115	0.707837	0.0008	34.17	3.13	0.710260
MLA 119	0.707747	0.0008	77.28	2.06	0.710260
MLA 119	0.707746	0.0008			0.710260
MLA 122	0.707803	0.0007	70.36	2.96	0.710260
MLA 126	0.707853	0.0007	77.07	2.33	0.710260
MLA 129	0.708039	0.0008	32.54	1.72	0.710260
MLA 130	0.708483	0.0009	38.10	1.11	0.710264
San Pedro del Rio					
MLA 475	0.707762	0.0006	26.01	1.82	0.710260
MLA 483	0.707837	0.0008	59.04	0.76	0.710260
MLA 491	0.707961	0.0007	18.97	2.06	0.710260
MLA 499	0.707809	0.0006	71.13	1.25	0.710260
MLA 507	0.707808	0.0009	19.25	2.85	0.710260
MLA 515	0.707868	0.0005	30.68	2.25	0.710260
MLA 523	0.707711	0.0008	20.28	0.89	0.710260
MLA 531	0.707681	0.0005	87.94	0.63	0.710260
MLA 539	0.707968	0.0008	28.77	1.04	0.710260
MLA 547	0.708012	0.0005	68.32	1.26	0.710260
MLA 555	0.707916	0.0006	17.47	1.87	0.710260
MLA 563	0.707752	0.0007	72.64	1.15	0.710260
MLA 571	0.707790	0.0005	30.67	2.27	0.710260
MLA 579	0.707766	0.0008	41.31	0.88	0.710260
MLA 587	0.708268	0.0008	54.53	0.70	0.710260
MLA 595	0.708021	0.0008	56.17	2.20	0.710260
MLA 603	0.707807	0.0007	49.82	1.08	0.710260
MLA 611	0.707899	0.0008	49.19	0.66	0.710260
MLA 619	0.707960	0.0008	58.49	0.49	0.710260
MLA 627	0.707956	0.0007	42.90	0.79	0.710260
MLA 635	0.707910	0.0007	37.75	0.53	0.710260
MLA 643	0.707813	0.0007	52.21	1.34	0.710260
MLA 651	0.707782	0.0006	62.59	2.22	0.710260
MLA 659	0.707914	0.0007	71.82	1.50	0.710260
MLA 667	0.708125	0.0006	9.57	0.67	0.710260
MLA 675	0.707933	0.0008	38.01	1.03	0.710260
MLA 683	0.707969	0.0007	39.90	4.06	0.710260
MLA 691	0.708276	0.0008	9.70	3.21	0.710260
MLA 697	0.710384	0.0008	10.11	3.24	0.710260

Note: TOC = total organic carbon.

CHAPTER NOTE*

N1. Sikora, P.J., and Bergen, J.A., submitted. Lower Cretaceous biostratigraphy of Ontong Java sites from DSDP Leg 30 and ODP Leg 192. *Spec. Publ.—Geol. Soc. London.*